

Vertical structure of the velocity field induced by mode-I and mode-II solitary waves in a stratified fluid*

Oxana Kurkina¹, Ekaterina Rouvinskaya¹, Andrey Kurkin¹, Ayrat Giniyatullin¹, and Efim Pelinovsky^{1,2,a}

¹ Laboratory of Modeling of Natural and Anthropogenic Disasters, Nizhny Novgorod State Technical University n.a. R.E. Alekseev, 24 Minin Str., 603950 Nizhny Novgorod, Russia

² Institute of Applied Physics, Russian Academy of Sciences, 46 Uljanov Str., 603950 Nizhny Novgorod, Russia

Received 24 September 2017

Published online: 30 March 2018 – © EDP Sciences / Società Italiana di Fisica / Springer-Verlag 2018

Abstract. The structure of the velocity field induced by internal solitary waves of the first and second modes is determined. The contribution from second-order terms in asymptotic expansion into the horizontal velocity is estimated for the models of almost two- and three-layer fluid for solitons of positive and negative polarity. The influence of the nonlinear correction manifests itself firstly in the shape of the lines of zero horizontal velocity: they are curved and the shape depends on the soliton amplitude and polarity, while for the leading-order wave field they are horizontal. Also the wave field accounting for the nonlinear correction for mode I has smaller maximal absolute values of negative velocities (near-surface for the soliton of elevation, and near-bottom for the soliton of depression) and larger maximums of positive velocities. For solitary waves of negative polarity, which are the most typical for hydrological conditions in the ocean for low and middle latitudes, the situation is the opposite. The velocity field of the mode-II soliton in a smoothed two-layer fluid reaches its maximal absolute values in a middle layer instead of near-bottom and near-surface maximums for mode-I solitons.

1 Introduction

Studies of nonlinear internal waves' (IWs) dynamics have quite a long history, originating in the first half of the twentieth century. Such waves have an influence on the hydrological regime of natural water bodies due to horizontal and vertical exchange, redistribution of heat, mixing of water, forming of the bottom topography etc. It is proved that such waves can create considerable loads and bending moments on the underwater parts of the offshore platforms, as well as contribute to the sediment resuspension. In the context of the impact on the environment internal solitary and breather-like waves are of greatest interest as the most intensive formations. Solitary waves are observed almost everywhere on the ocean shelves and they are clearly visible on satellite images [1].

The shapes and properties of these waves are studied well enough in the framework of various theoretical models, in particular within the weakly nonlinear theory of long waves, represented by the Korteweg-de Vries equation and its extended versions, such as the Gardner equation, the modified Korteweg-de Vries equation, “2 + 4” Korteweg-de Vries equation [2], and others. In the major-

ity of classical studies devoted to internal solitary waves emphasis placed on the dynamics of such waves during the propagation over a rough bottom (see, *e.g.*, paper [3], dedicated to the transformation of solitons over a sloping bottom and the paper [4] devoted to the dynamics of breather-like waves in the shelf zone of the Baltic sea), the interaction of such waves, or estimation of such local characteristics, as near-bottom and near-surface velocity and pressure variations at the bottom and on the pillars induced by the propagating waves. However, it is necessary to represent the structure of the velocity field in the entire water column for a more complete understanding of what is happening in the ocean during the propagation of internal solitary waves. Some peculiarities of the internal solitary waves' spatial structure are investigated in the framework of the Korteweg-de Vries equation [5] and the modified Korteweg-de Vries equation for the ocean with two pycnoclines [6].

In the present paper we briefly describe the governing equations of a weakly nonlinear theoretical model for internal waves of different vertical modes (sect. 2). Then we give the detailed description of the vertical structure, 2D fields (vertical plane) of horizontal velocity, its nonlinear correction and vorticity for mode-I and mode-II internal solitary waves with moderate amplitude in a quasi-two-layer (sect. 3) and a quasi-three-layer (sect. 4) fluid. The results are discussed and conclusions are given in sect. 5.

* Contribution to the Topical Issue “Non-equilibrium processes in multicomponent and multiphase media” edited by Tatyana Lyubimova, Valentina Shevtsova, Fabrizio Crocco.

^a e-mail: pelinovsky@gmail.com

2 Theoretical model

The weakly nonlinear theory of long IWs in a vertical section of stratified basin assumes that the internal wave field (in particular, the vertical isopycnal displacement $\zeta(z, x, t)$) can be expressed as a series (up to the 2nd order in amplitude) [7]:

$$\zeta(z, x, t) = \eta(x, t)\Phi(z) + \eta^2(x, t)F(z), \quad (1)$$

where x is horizontal axis, z is vertical axis directed upwards, t is time, $\eta(x, t)$ describes the wave propagation along the axis of propagation and its evolution in time. Function $\Phi(z)$ (the vertical mode) describes the vertical structure of the long linear internal wave, and $F(z)$ is the first nonlinear correction to $\Phi(z)$. $\Phi(z)$ is a solution of an eigenvalue problem, which can be written in the form (in Boussinesq approximation usually valid for natural sea stratifications):

$$\frac{d^2\Phi}{dz^2} + \frac{N^2(z)}{c^2}\Phi = 0, \quad \Phi(0) = \Phi(H) = 0. \quad (2)$$

Here the eigenvalue c is the phase speed of the long linear internal wave, H is the total water depth, $N(z)$ is the Brunt-Väisälä frequency determined by the expression

$$N^2(z) = -\frac{g}{\rho(z)} \frac{d\rho(z)}{dz}, \quad (3)$$

g is the gravity acceleration and $\rho(z)$ is the undisturbed density profile. It is well known that problem (2) has an infinite number of eigenvalues $c_1 > c_2 > c_3 > \dots$ and corresponding eigenfunctions $\Phi_1, \Phi_2, \Phi_3, \dots$. Though there is a number of ways to normalize the solution for high modes, it is convenient to do this in such a way that the first extremum, counting from the surface, is equal to 1: $\Phi(z_{\max}) = 1$ [8].

In this case the leading-order solution $\eta(x, t)$ coincides with the isopycnal surface displacement at z_{\max} :

$$\zeta(x, z_{\max}, t) = \eta(x, t). \quad (4)$$

The function $F(z)$ can be found as a solution of the inhomogeneous boundary problem:

$$\begin{cases} \frac{d^2F}{dz^2} + \frac{N^2}{c^2}F = -\frac{\alpha}{c} \frac{d^2\Phi}{dz^2} + \frac{3}{2} \frac{d}{dz} \left[\left(\frac{d\Phi}{dz} \right)^2 \right], \\ F(0) = F(H) = 0, \end{cases} \quad (5)$$

A unique solution for eq. (5) can be obtained using an additional normalising condition $F(z_{\max}) = 0$.

In this model, the function $\eta(x, t)$ satisfies the nonlinear evolution equation (extended Korteweg-de Vries (KdV) or Gardner equation):

$$\frac{\partial\eta}{\partial t} + (c + \alpha\eta + \alpha_1\eta^2) \frac{\partial\eta}{\partial x} + \beta \frac{\partial^3\eta}{\partial x^3} = 0. \quad (6)$$

This equation compared to the classic KdV equation contains cubic nonlinearity, the presence of which provides better predictions of the wave form, especially in

the coastal zone. The coefficients of this equation are determined through the $\Phi(z)$ and $F(z)$:

$$\begin{aligned} \beta &= \frac{c \int_0^H \Phi^2 dz}{2 \int_0^H \left(\frac{d\Phi}{dz} \right)^2 dz}, & \alpha &= \frac{3c \int_0^H \left(\frac{d\Phi}{dz} \right)^3 dz}{2 \int_0^H \left(\frac{d\Phi}{dz} \right)^2 dz}, \\ \alpha_1 &= \frac{1}{2 \int_0^H \left(\frac{d\Phi}{dz} \right)^2 dz} \int_0^H dz \left\{ 9c \frac{dF}{dz} \left(\frac{d\Phi}{dz} \right)^2 - 6c \left(\frac{d\Phi}{dz} \right)^4 \right. \\ &\quad \left. + 5\alpha \left(\frac{d\Phi}{dz} \right)^3 - 4\alpha \frac{dF}{dz} \frac{d\Phi}{dz} - \frac{\alpha^2}{c} \left(\frac{d\Phi}{dz} \right)^2 \right\}. \end{aligned} \quad (7)$$

Let us consider the single-soliton solution of eq. (6):

$$\eta(x, t) = \frac{A}{1 + B \operatorname{ch}(\gamma(x - Vt))}, \quad (8)$$

where the soliton velocity $V = c + \beta\gamma^2$ is expressed through the inverse width of the soliton, γ , and the soliton amplitude, a , or the extremum of the function (8), is

$$A = a(1 + B), \quad \gamma^2 = \frac{A\alpha}{6\beta}, \quad B^2 = 1 + \frac{6\alpha_1\beta\gamma^2}{\alpha^2}. \quad (9)$$

When the cubic nonlinear coefficient α_1 is negative, soliton solutions of single polarity, with $\alpha\eta > 0$, exist with amplitudes between zero and a limiting value

$$a_{\lim} = \frac{\alpha}{|\alpha_1|}. \quad (10)$$

With the use of eq. (1) the components of the velocities of particles (u, w) in the vertical section (x, z) can be expressed as follows:

$$\begin{cases} u(x, z, t) = u_l + u_n, \\ u_l = c\eta(x, t) \frac{d\Phi}{dz}, \quad u_n = \left(\frac{\alpha}{2} \frac{d\Phi}{dz} + c \frac{dF}{dz} \right) \eta^2, \end{cases} \quad (11)$$

$$\begin{cases} w(x, z, t) = w_l + w_n, \\ w_l = -c \frac{\partial\eta}{\partial x} \Phi(z), \quad w_n = -(\alpha\Phi(z) + 2cF(z))\eta \frac{\partial\eta}{\partial x}. \end{cases} \quad (12)$$

The horizontal velocity component u gives the greatest contribution into the local current speed. This is typical for long waves and this characteristic of the internal wave field must be considered in the analysis of near-bottom processes connected with the sediment transport. The first terms in eqs. (11) and (12) correspond to the leading order of the asymptotic expansion. The remaining additives result from the first nonlinear correction in the asymptotic series. Thus, for the forecast of the local current speed one has to determine the isopycnal displacement $\eta(x, t)$ at the level of z_{\max} (see (5)), the vertical IW mode $\Phi(z)$ and its nonlinear correction $F(z)$. The amplitude of $\eta(x, t)$ is not known *a priori*, it depends upon a large number of background conditions of internal wave generation, and can be found by means of the detailed simulation.

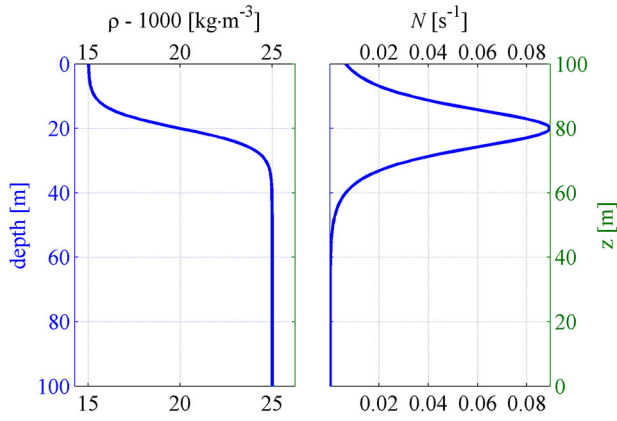


Fig. 1. Left panel: model vertical profile of the sea water density; right panel: Brunt-Väisälä frequency.

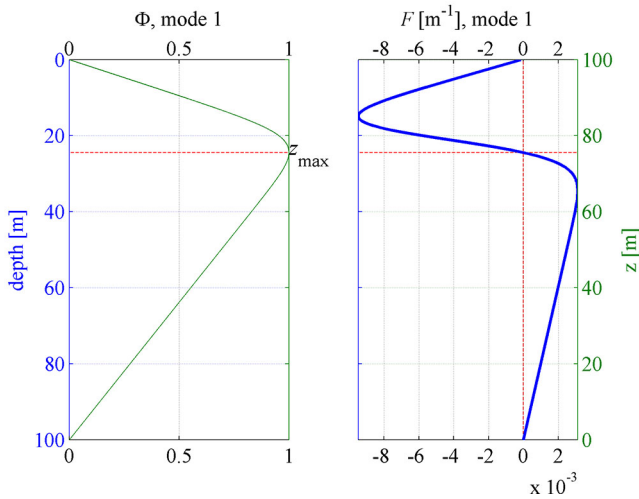


Fig. 2. Left panel: typical form of the first linear mode function for internal waves; right panel: nonlinear correction to it.

3 IWs in quasi-two-layer fluid

The structure of the linear part and the contribution of the correction terms to the horizontal velocity can be estimated for the model stratification. A typical density stratification profile is taken as a two-layer fluid with a smooth density change on the pycnocline

$$\rho(z) = \frac{\Delta\rho}{2} \text{th} \frac{z - z_p}{w_p}, \quad (13)$$

where $\Delta\rho$ is the value of the density “jump” (assumed here equal to 10 kg/m^3), z_p is the position of the “jump” center along the vertical (here it corresponds to 20 m from the surface, with a total depth of 100 m), w_p is the typical width of the “jump” along the vertical coordinate (here it is equal 6 m). This profile of the fluid density and the vertical profile of the Brunt-Väisälä frequency are shown in fig. 1.

The computed function $\Phi(z)$ and the nonlinear correction $F(z)$ for the first (lowest) mode are shown in fig. 2 for such density stratification. The coefficients of the Gardner

Table 1. The coefficients of the Gardner equation for internal waves of the first and second modes.

Mode number	1	2
c [m/s]	1.13	0.32
β [m^3/s]	357	18
α [s^{-1}]	-0.006	0.007
α_1 [$\text{m}^{-1} \cdot \text{s}^{-1}$]	-0.0018	0.0017

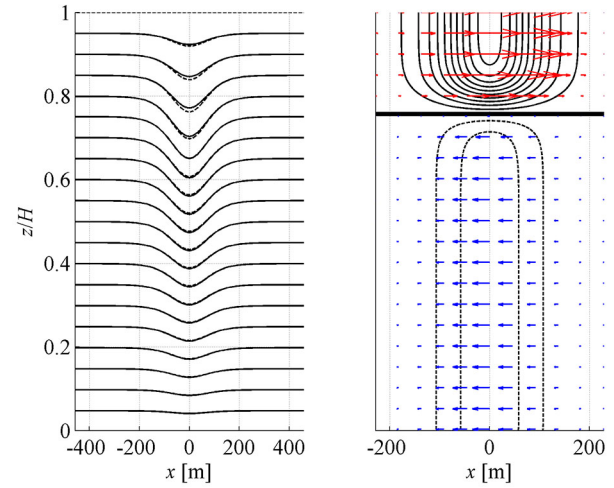


Fig. 3. Left panel: wave field represented as a vertical displacement of isopycnic lines at different horizons, for the first mode soliton with the amplitude equal to 10 m (the solid lines are the linear component, the dashed lines are vertical displacements with consideration of the nonlinear correction). Right panel: the horizontal velocity field corresponding to a linear wave field on the left panel (the bold solid line is the isoline corresponding to the zero velocity value; thin solid lines are the isolines of positive values; the dashed lines are the contours of negative values; the interval between the contours corresponds to $0.05c$).

equation (6) under such background conditions for two modes are given in table 1.

It can be noted that for the first mode both nonlinear coefficients α and α_1 are negative and in such a fluid only solitons of negative polarity bounded by the limiting amplitude $a_{\text{lim}} = -33.3 \text{ m}$ can exist.

The contours of equal density (isopycnic lines) and the contours of the horizontal velocity in the linear approximation for the internal solitary wave of the first mode with an amplitude equal to $H/10 = 10 \text{ m}$ are shown in fig. 3.

The spatial structure of the nonlinear correction to the horizontal velocity and its total field are shown in fig. 4. These figures demonstrate a quasi-two-layer structure of the horizontal velocity with a thin transition layer of width $2w_p$. The particle velocity is considered positive when the direction of its motion coincides with the direction of the soliton’ propagation (here it is the direction of the positive values of the horizontal axis). For the chosen density stratification, the particle velocities for a negative-polarity

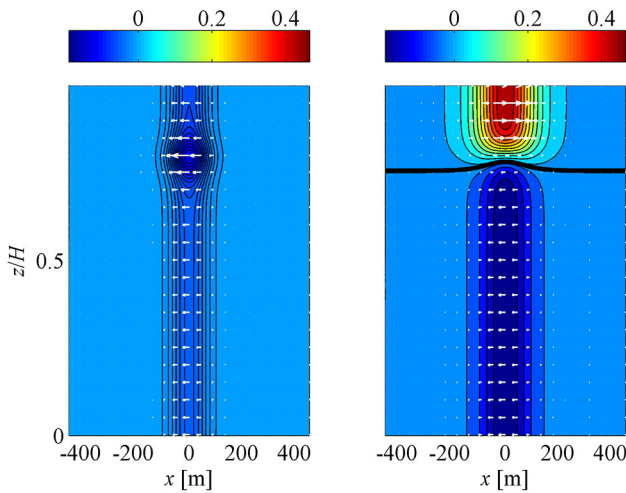


Fig. 4. Left panel: nonlinear correction to the horizontal velocity; right panel: field of the horizontal velocity with consideration of nonlinear correction for the internal solitary wave of the first mode. (Solid line: isoline, corresponding to the zero velocity value; the interval between the contours corresponds to $0.05c$.) Both characteristics are normalized to the phase velocity c of the first mode.

soliton are positive in the upper layer and negative in the lower layer.

The velocities in the upper and lower layers reach the maximum absolute values at the surface and at the bottom of the fluid, respectively. The influence of the nonlinear correction is manifested primarily in the form of an isoline of zero horizontal velocity (shown in bold in fig. 4): it is a horizontal line in the linear approximation (fig. 3, right), but when the nonlinear correction is taken into account, it becomes curved. Its curvature and polarity depend on the soliton amplitude. Accounting for the nonlinear correction also leads to a slight increase in the absolute values of the particle velocity near the bottom and to an insignificant decrease in near-surface velocities. Thus, the linear part of the horizontal velocity in (11) gives an upper estimate for the flow velocity at the surface and a lower estimate for the bottom.

The vertical structure of the second mode and its nonlinear correction $F(z)$ are shown in fig. 5. The function $\Phi(z)$ vanishes once inside the interval $(0, H)$ in this case. As one can see from table 1, both nonlinear coefficients are positive for the second mode. In this case, there are two families of soliton solutions: the first one with positive polarity, for which there is no upper or lower amplitude limitation, and the second family with negative polarity, for which the absolute value of the amplitude should be greater than the modulus of the amplitude of the algebraic soliton ($a_{\text{alg}} = -2\alpha/\alpha_1$).

The displaced isopycnic lines and the contours of the horizontal velocity in the linear approximation during the propagation of the internal solitary wave of the second mode with an amplitude of $H/20 = 5$ m (having a positive polarity at the maximum of the linear mode) are shown in

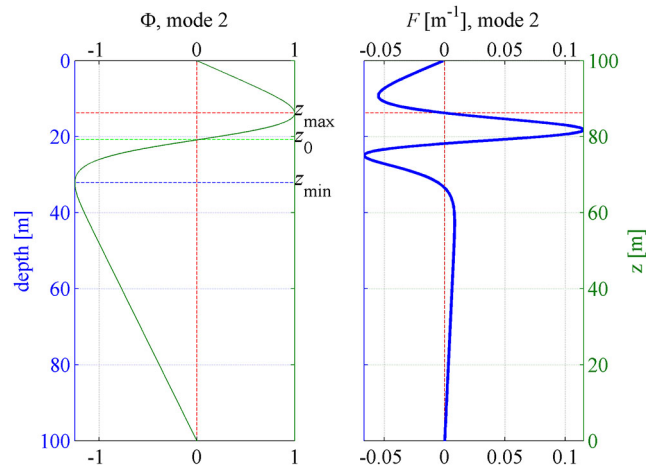


Fig. 5. Structure of the second linear mode function for internal waves (left); nonlinear correction (right).

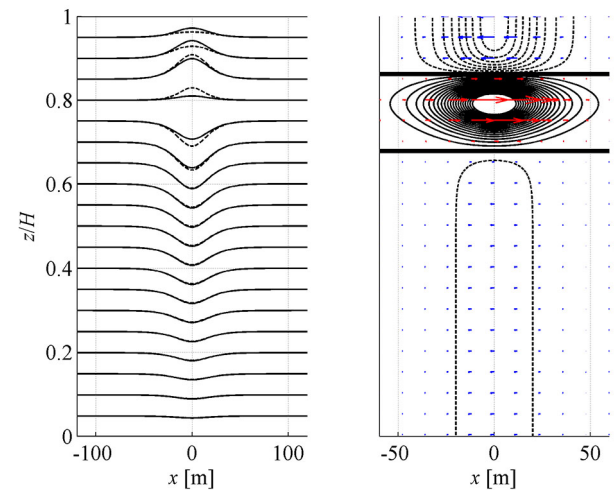


Fig. 6. Left panel: wave field represented as a vertical displacement of isopycnic lines at different horizons, for the second-mode soliton with an amplitude equal to $H/20$ (the solid lines are the linear component, the dashed lines are the vertical displacements with consideration of the nonlinear correction). Right panel: the horizontal velocity field corresponding to a linear wave field on the left panel (the bold solid line is the isoline corresponding to the zero velocity value, thin solid lines are the isolines of positive values, the dashed lines are the contours of negative values; the interval between the contours corresponds to $0.05c$).

fig. 6. Such solitary waves of the second mode are usually called “convex” [9].

The nonlinear correction to the horizontal velocity and its total value for an internal solitary wave of second mode are shown in fig. 7. Maximal absolute values of the horizontal velocity are positive located inside the fluid. The range of positive and negative velocity values is asymmetric with respect to zero (the maximal absolute values of negative velocities are much less than the maximal posi-

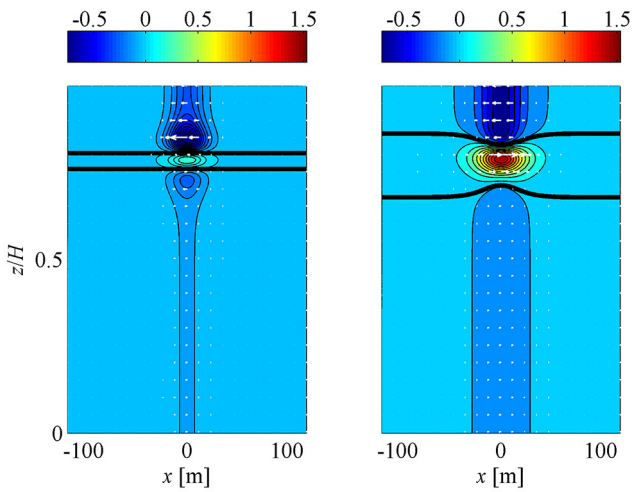


Fig. 7. Left panel: nonlinear correction to horizontal velocity. Right panel: field of the horizontal velocity with consideration of the nonlinear correction for the internal solitary wave of the second mode. Both characteristics are normalized to the phase velocity c of the second mode.

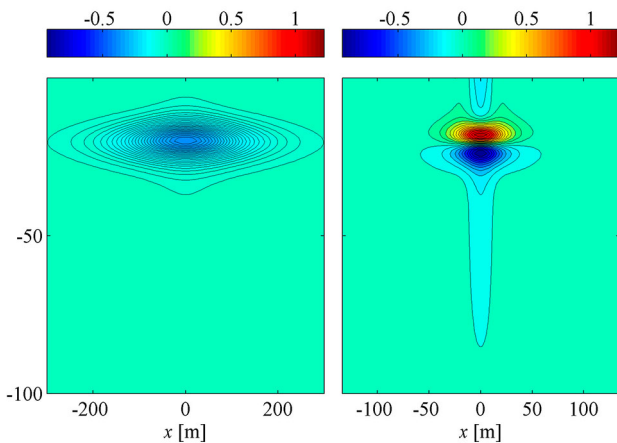


Fig. 8. Left panel: vorticity for the internal solitary wave of the first mode, shown in fig. 2. Right panel: vorticity for the internal solitary wave of the second mode, shown in fig. 6. Vorticity is normalized to the maximal value of the Brunt-Väisälä frequency (fig. 1).

tive velocities’ values). Near-bottom and near-surface velocities are small in relation to velocities in the “middle” layer of the fluid and they are negative. There are two lines of zero velocity in the water column. Taking into account the nonlinear correction for the vertical structure of the mode leads to their bending.

The vorticity (see, *e.g.* [10]) for internal solitary waves of the first and second mode is shown in fig. 8. It is normalized to the maximal value of the Brunt-Väisälä frequency $N(z)$. As we can see from this graph, vorticity for the first-mode solitary wave is negative and its absolute values reach $0.4N_{\max}$. The vorticity for the second-mode solitary wave has both positive and negative values in the interval $[-0.9N_{\max}; 1.2N_{\max}]$.

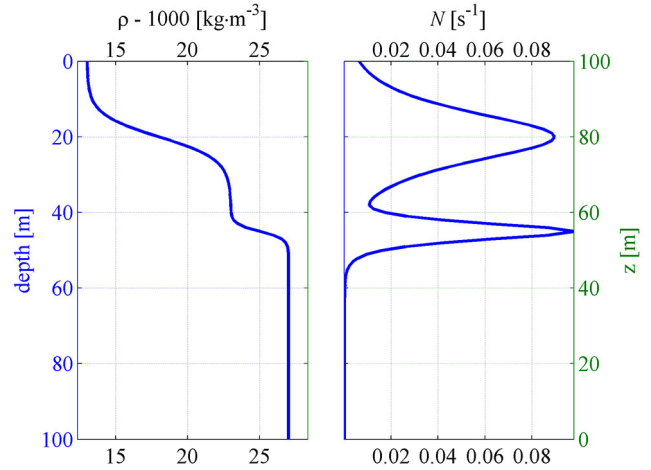


Fig. 9. Left panel: model vertical profile of a three-layer fluid; right panel: Brunt-Väisälä frequency.

Table 2. The coefficients of the Gardner equation for internal waves of the first and second modes in the three-layer fluid.

Mode number	1	2
c [m/s]	1.34	0.64
β [m ³ /s]	563	66.8
α [s ⁻¹]	-0.045	0.0595
α_1 [m ⁻¹ · s ⁻¹]	0.00014	-0.0065

4 IWs in quasi-three-layer fluid

It is obvious that the spatial structure of the velocity field of a solitary wave will differ substantially for both modes if we will use, for example, a three-layer model for which the wave regimes in the framework of the Gardner equation were studied in detail in [5].

The profile of the density for a three-layer fluid and the vertical profile of the Brunt-Väisälä frequency for such a fluid are shown in fig. 9.

The coefficients of the Gardner equation (6) under such background conditions are given in table 2.

The function $\Phi(z)$ and the nonlinear correction $F(z)$ for the first mode are shown in fig. 10 for such density stratification.

The contours of equal density and the contours of the horizontal velocity in the linear approximation during the propagation of the internal solitary wave of the first mode with an amplitude of $-H/10$ are shown in fig. 11.

The structure of the isopycnal displacement field and the field of horizontal velocity for the soliton of the first mode in the selected three-layer fluid are qualitatively similar to those for the soliton of the first mode in a two-layer fluid. The spatial structure of the nonlinear correction to the horizontal velocity and its total value for such a case are shown in fig. 12. Here we can also see a qualitative agreement with the results presented in fig. 4.

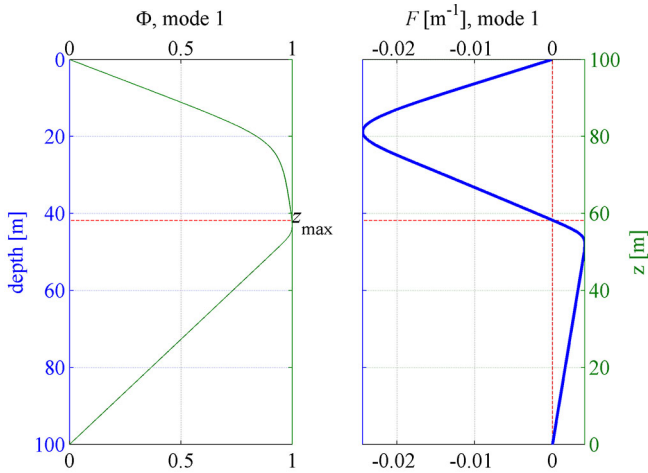


Fig. 10. Left panel: typical form of the first linear mode function for internal waves in a three-layer fluid; right panel: nonlinear correction to it.

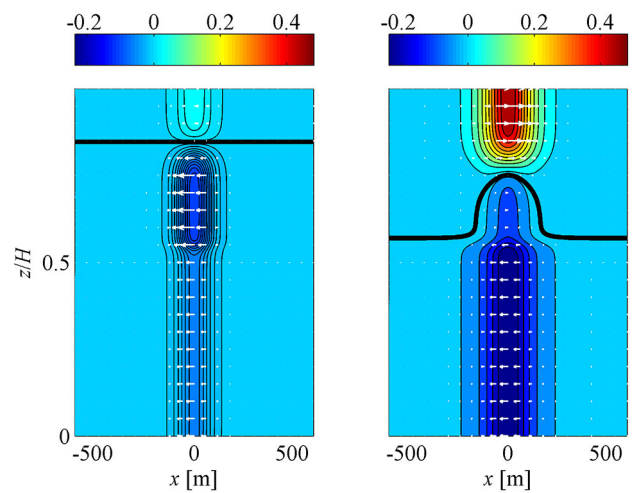


Fig. 12. Left panel: nonlinear correction to the horizontal velocity; right panel: field of the horizontal velocity with consideration of the nonlinear correction for the internal solitary wave of the first mode. (Solid line: isoline, corresponding to the zero velocity value; the interval between the contours corresponds to $0.05c$.)

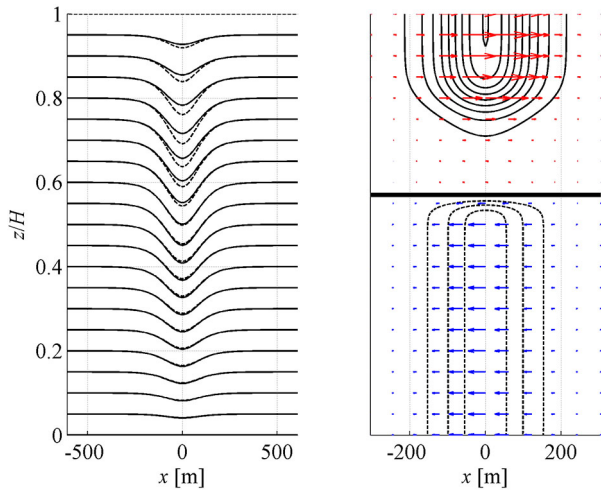


Fig. 11. Left panel: wave field represented as a vertical displacement of isopycnic lines at different horizons, for the first-mode soliton with an amplitude equal to $-H/10$ (the solid lines are the linear component, the dashed lines are the vertical displacements with consideration of the nonlinear correction). Right panel: the horizontal velocity field corresponding to a linear wave field on the left panel (the bold solid line is the isoline corresponding to the zero velocity value, thin solid lines are the isolines of positive values, the dashed lines are the contours of negative values; the interval between the contours corresponds to $0.05c$).

The vertical structure of the second mode and the first nonlinear correction to it are shown in fig. 13 for a three-layer fluid.

The displaced isopycnic lines and the contours of the horizontal velocity in the linear approximation during the propagation of the internal solitary wave of the second mode with an amplitude of $H/20$ that has a positive polarity at the maximum of the linear mode (this wave is also of convex type) are shown in fig. 14. The spatial structure

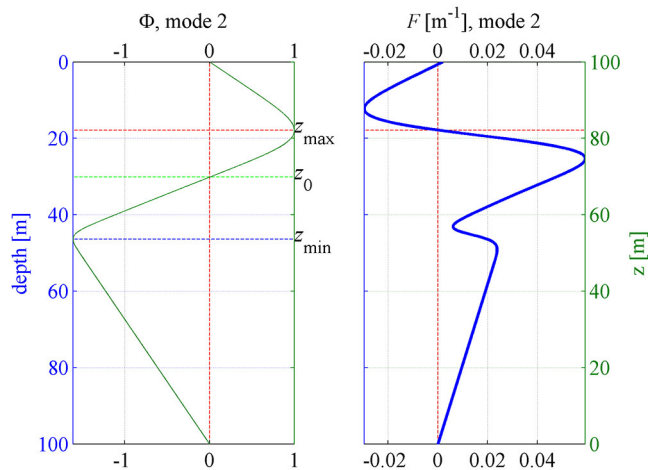


Fig. 13. Left panel: typical form of the second linear mode function for internal waves in a three-layer fluid; right panel: nonlinear correction to it.

of the horizontal velocity for an internal solitary wave of the second mode in a three-layer fluid is shown in fig. 15 in detail. From these figures, we can see that the spatial structure of the horizontal velocity field and the field of isopycnal displacements induced by an internal solitary wave of the second mode are qualitatively similar in a two- and three-layer fluid. Maximal absolute values of the horizontal velocity are obtained in the mid-layer and near the surface for this example. The spatial structure of the nonlinear correction to the horizontal velocity in a three-layer fluid differs markedly from such a nonlinear correction in a two-layer fluid.

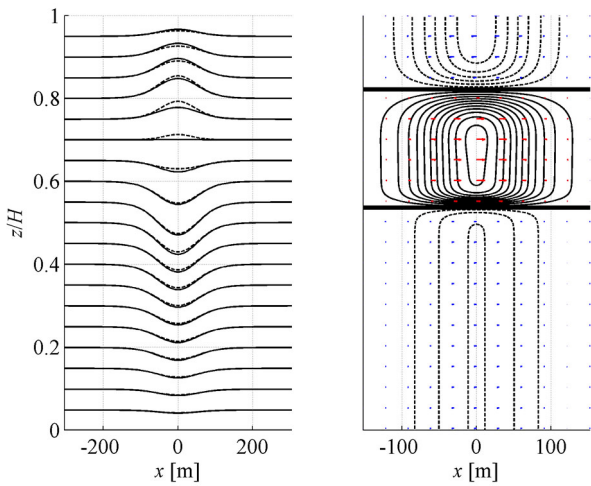


Fig. 14. Left panel: wave field represented as a vertical displacement of isopycnic lines at different horizons, for the second-mode soliton with an amplitude equal to $H/20$ (the solid lines are the linear component, the dashed lines are the vertical displacements with consideration of the nonlinear correction). Right panel: the horizontal velocity field corresponding to a linear wave field on the left panel (the bold solid line is the isoline corresponding to the zero velocity value, thin solid lines are the isolines of positive values, the dashed lines are the contours of negative values; the interval between the contours corresponds to $0.05c$).

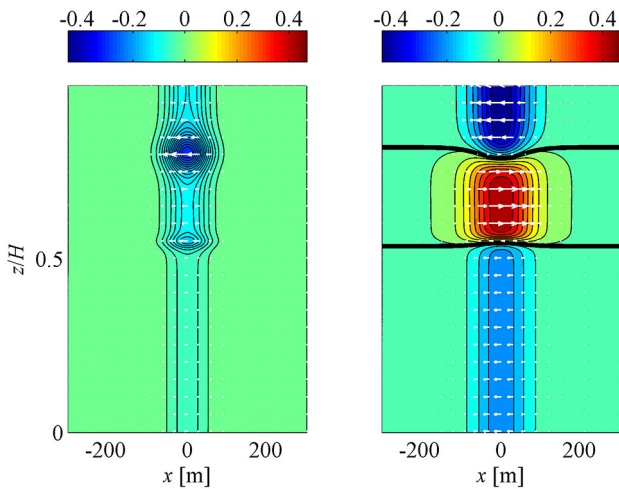


Fig. 15. Left panel: nonlinear correction to the horizontal velocity in the three-layer fluid. Right panel: field of the horizontal velocity with consideration of the nonlinear correction for the internal solitary wave of the second mode. Both characteristics are normalized to the phase velocity of the second mode.

The vorticity for internal solitary waves of the first and second mode in the quasi-three-layer fluid is shown in fig. 16. The features of the distribution of this characteristic for the first and second modes in the quasi-three-layer fluid are in many respects similar to those for internal waves of the first and second modes in the quasi-two-layer fluid.

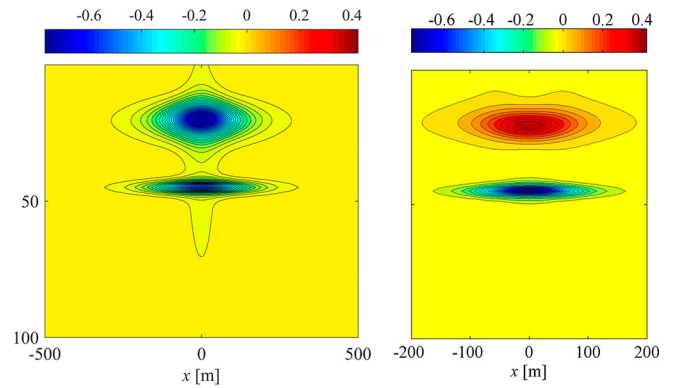


Fig. 16. Left panel: vorticity for the internal solitary wave of the first mode (fig. 11). Right panel: vorticity for the internal solitary wave of the second mode (fig. 14). Vorticity is normalized to the maximal value of the Brunt-Väisälä frequency in the quasi-three-layer fluid (fig. 9).

5 Conclusion

The structure of the velocity field induced by internal solitary waves of the first and second modes in a quasi-two- and -three-layer fluid is investigated in the framework of the weakly nonlinear theory of ideal fluid. We show that nonlinear corrections in the asymptotic series are important and lead to additional values of the velocities near the sea surface, influencing the satellite images of internal waves from space. Similarly, accounting for the nonlinear correction of velocities in the near-bottom layer results into the intensification of the sediment transport.

We would like also to mention that the thickness of the pycnocline(s) is rather small in the considered models of density stratification. As a result, the horizontal velocity of the current in the soliton varies in a jump-like manner in the pycnocline(s), providing the conditions for the development of a Kelvin-Helmholtz instability and turbulence of the current in the case when the viscosity is taken into account [11]. Turbulent processes in the pycnocline and the near-bottom layer will influence particle transport, and here nonlinear corrections to the velocity field should be also accounted.

The results were obtained in the framework of the state task programme in the sphere of the scientific activity of the Ministry of Education and Science of the Russian Federation (projects No. 5.4568.2017/6.7 and No. 5.1246.2017/4.6) and with the support of the Russian President’s scholarship for young scientists and graduate students SP-2311.2016.5.

Author contribution statement

OK conceived the study, developed the theoretical background and contributed to writing the calculation code. ER and AG designed the computational framework and performed the calculations. AK was in charge of overall direction and planning and wrote the manuscript with input from all authors. EP contributed in the nonlinear theory of internal waves. All authors discussed the results and provided critical feedback.

References

1. C.R. Jackson, *An Atlas of Internal Solitary-like Waves and Their Properties*, 2nd edition (Global Ocean Associates, 2004).
2. O.E. Kurkina *et al.*, JETP Lett. **95**, 91 (2012).
3. T.G. Talipova *et al.*, Izv. Atmos. Ocean. Phys. **51**, 89 (2015).
4. E. Rouvinskaya, Cont. Shelf Res. **110**, 60 (2015).
5. V. Vlasenko, P. Brandt, A. Rubino, J. Phys. Oceanogr. **30**, 2172 (2000).
6. E. Rouvinskaya, O. Kurkina, A. Kurkin, Bulletin of Moscow State Regional University, Series “Physics and Mathematics” Vol. **2** (2011) p. 61.
7. E. Pelinovsky *et al.*, *Solitary Waves in Fluids* (WIT Press, Boston, Southampton, 2007) Chapt. 4.
8. O. Kurkina *et al.*, Nonlinear Process. Geophys. **24**, 645 (2017).
9. Y.J. Yang *et al.*, Nonlinear Process. Geophys. **17**, 605 (2010).
10. O. Kurkina *et al.*, Nonlinear Process. Geophys. **22**, 117 (2015).
11. O.E. Kurkina *et al.*, Oceanology **56**, 767 (2016).